

# EPR study of fine and hyperfine interactions of $\text{Gd}^{3+}$ in $\text{Bi}_{2(1-x)}\text{Gd}_{2x}\text{Se}_3$ and $\text{Pb}_{1-x}\text{Gd}_x\text{Se}$

Xavier Gratens, Samih Isber,\* Salam Charar, Claude Fau, and Michel Averous

Groupe d'Etude des Semiconducteurs URA 357, Université Montpellier II, Place Eugène Bataillon, 34095 Montpellier Cedex 5, France

Sushil K. Misra

Department of Physics, Concordia University, 1455 de Maisonneuve Boulevard West, Montreal, Quebec, Canada H3G 1M8

Zbigniew Golacki

Institute of Physics, Polish Academy of Sciences, Pl. 02-668, Warsaw, Poland

Marhoun Ferhat and Jean C. Tedenac

Laboratoire de Physiochimie des Matériaux Solides, Université Montpellier II, Place Eugène Bataillon, 34095 Montpellier Cedex 5, France

(Received 12 August 1996; revised manuscript received 20 November 1996)

Electron paramagnetic resonance experiments were performed on  $\text{Bi}_{2(1-x)}\text{Gd}_{2x}\text{Se}_3$  and  $\text{Pb}_{1-x}\text{Gd}_x\text{Se}$  samples at room and liquid-helium temperatures. The  $\text{Gd}^{3+}$  sites are characterized by hexagonal and octahedral symmetries in  $\text{Bi}_{2(1-x)}\text{Gd}_{2x}\text{Se}_3$  and  $\text{Pb}_{1-x}\text{Gd}_x\text{Se}$  samples, respectively. The absolute signs of the spin-Hamiltonian parameters in  $\text{Bi}_{2(1-x)}\text{Gd}_{2x}\text{Se}_3$  were determined by comparing the intensities of the lines at room and liquid-helium temperatures:  $b_2^0 < 0$ ,  $b_4^0 > 0$ , and  $b_6^0 < 0$ . The  $|b_2^0|$  value in  $\text{Bi}_{2(1-x)}\text{Gd}_{2x}\text{Se}_3$  increased nonlinearly with decreasing temperature, becoming constant below 40 K. At the low temperature of 2.2 K, four hyperfine transitions due to the  $^{155}\text{Gd}$  isotope ( $I = 3/2$ ) were observed in  $\text{Pb}_{1-x}\text{Gd}_x\text{Se}$ , leading to the average value of the hyperfine-coupling constant of  $2.55 \pm 0.10$  mT for the two  $^{155}\text{Gd}$  and  $^{157}\text{Gd}$  processing nonzero nuclear magnetic moments. [S0163-1829(97)08109-5]

## I. INTRODUCTION

Many researches involving electron paramagnetic resonance (EPR) and magnetic properties on diluted magnetic semiconductors have been reported in the literature.<sup>1-5</sup> Recently, some of us published studies on magnetic properties of  $\text{Bi}_{2(1-x)}\text{Ge}_{2x}\text{Te}_3$  ( $x = 0.01$ ).<sup>6,7</sup> It was found that the magnetizations at 4.2 and 1.8 K fit very well with contributions both from isolated  $\text{Gd}^{3+}$  ions and their pairs. The exchange interaction between the  $\text{Gd}^{3+}$  ions was determined to be antiferromagnetic, with the value  $J_p/k_B = -0.5$  K.

$\text{Bi}_2\text{Te}_3$  and  $\text{Bi}_2\text{Se}_3$  single crystals are semiconductors, characterized by small indirect gaps  $E_g = 150$  and  $160$  meV for  $\text{Bi}_2\text{Te}_3$  and  $\text{Bi}_2\text{Se}_3$ , respectively.<sup>8</sup> Both these materials possess rhombohedral structure ( $R\bar{3}m$ ).<sup>7,8</sup> The characteristic cleavage planes result due to the shorter interlayer bond lengths between the Se atoms. The layers alternate in the following sequence of planes perpendicular to a threefold axis:  $\text{Se}^{(1)}\text{-Bi-Se}^{(2)}\text{-Bi-Se}^{(1)}$ . As for PbSe, it is a IV-VI semiconductor, characterized by a small gap  $E_g = 300$  meV at room temperature.<sup>9-11</sup>

Recently, magnetization measurements on rare-earth-ion-doped PbSe ( $\text{Eu}^{2+}$ ,  $\text{Gd}^{3+}$ ) samples were reported.<sup>2,12,13</sup> In this material, the first-nearest-neighbor exchange interaction is the dominant one. The exchange interactions among the rare-earth ions in IV-VI semiconductors are much smaller in comparison to those characterizing II-VI semiconductors. A recent low-temperature magnetization measurement on three samples of  $\text{Pb}_{1-x}\text{Eu}_x\text{Se}$  ( $x = 1.3\%$ ,  $3.0\%$ , and  $4.1\%$ ) revealed the existence of an antiferromagnetic exchange constant  $J_1/k_B = -0.24 \pm 0.02$  K between the  $\text{Eu}^{2+}$  ions.<sup>2</sup> Mag-

netization steps due to single-ion anisotropy of the  $\text{Eu}^{2+}$  ion in PbSe confirmed the positive absolute sign of  $b_4^0$ . In addition, the value of  $b_4^0$  so estimated was found to be in good agreement with that estimated by EPR.<sup>1</sup> The first EPR studies on  $\text{Pb}_{1-x}\text{Gd}_x\text{Se}$  were performed by Bacskey *et al.*<sup>14</sup> at room temperature. In this paper, room- and liquid-helium-temperature EPR measurements on the  $\text{Gd}^{3+}$  ion incorporated in  $\text{Bi}_2\text{Se}_3$  and PbSe samples are presented.

## II. SAMPLE PREPARATION AND EXPERIMENTAL ARRANGEMENT

$\text{Bi}_{2(1-x)}\text{Gd}_{2x}\text{Te}_3$  and  $\text{Pb}_{1-x}\text{Gd}_x\text{Se}$  samples were prepared by the well-known Bridgman technique. Mixtures of constituting elements, each of 99.999% purity, were used in a sealed evacuated quartz ampoule at a constant temperature of  $850^\circ\text{C}$  for 72 h. The Bridgman apparatus was characterized by a temperature gradient of about  $20^\circ\text{C}/\text{cm}$ . The unit-cell parameters were determined by x-ray diffraction for hexagonal  $\text{Bi}_2\text{Se}_3$  to be  $a = 4.14$  Å and  $c = 28.7$  Å, and, for cubic PbSe,  $a = 6.12$  Å. The microprobe analysis revealed the concentration ( $x$ ) of  $\text{Gd}^{3+}$  ions to be 0.12% and 1.04% in  $\text{Bi}_{2(1-x)}\text{Gd}_{2x}\text{Te}_3$  and  $\text{Pb}_{1-x}\text{Gd}_x\text{Se}$ , respectively. A Bruker spectrometer (9.58 GHz) equipped with an Oxford helium-gas-flow cryostat to attain liquid-helium temperatures and a Varian spectrometer (9.14 GHz) equipped with a commercial (Andonian) helium-immersion cryostat, wherein the temperature 2.2 K was obtained by pumping on liquid helium were used for EPR measurements. The  $\text{Bi}_{2(1-x)}\text{Gd}_{2x}\text{Se}_3$  sample, with approximate dimensions  $0.5 \times 2 \times 4$  mm<sup>3</sup>, was placed in an evacuated, sealed quartz tube.

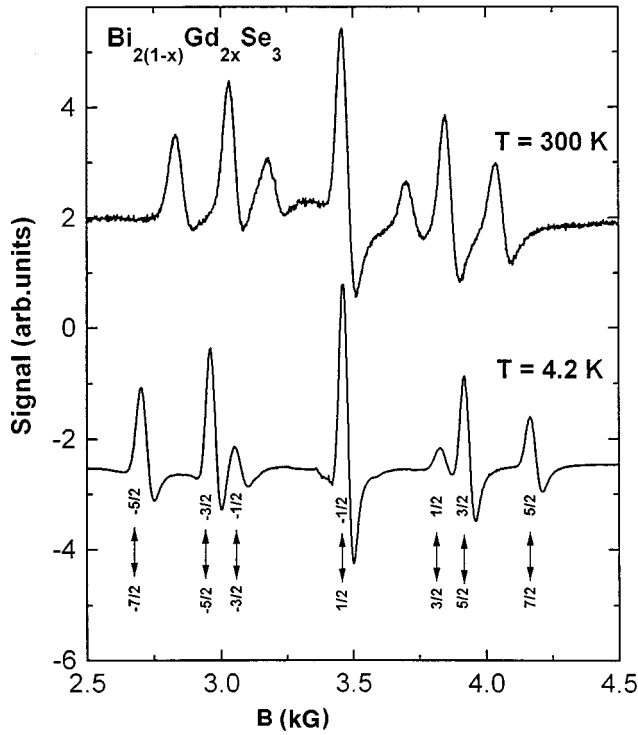


FIG. 1. X-band (9.57 GHz) EPR spectra of  $\text{Bi}_{2(1-x)}\text{Gd}_{2x}\text{Se}_3$  at 300 and 4.2 K, the external magnetic field being parallel to the  $c$  axis. The difference in the overall splittings at the two temperatures can be clearly seen.

### III. EXPERIMENTAL RESULTS AND DISCUSSION

#### A. $\text{Gd}^{3+}$ in $\text{Bi}_2\text{Se}_3$

##### 1. Spin Hamiltonian and line positions

The  $\text{Gd}^{3+}$  spin Hamiltonian appropriate to the hexagonal site symmetry in  $\text{Bi}_2\text{Se}_3$  and assuming an isotropic  $g$  matrix, since the departures from isotropic symmetry are small is given, in the usual notation by<sup>15–18</sup>

$$\mathcal{H} = g\mu_B \mathbf{B} \cdot \mathbf{S} + \frac{1}{3}b_2^0 O_2^0 + \frac{1}{60}(b_4^0 O_4^0 + b_4^3 O_4^3) + \frac{1}{1260}(b_6^0 O_6^0 + b_6^3 O_6^3 + b_6^6 O_6^6). \quad (1)$$

The positions of the lines to second order in perturbation for  $\mathbf{B}$  parallel to the hexagonal axis are given in Refs. 15–17.

##### 2. EPR spectra

The EPR spectrum of  $\text{Bi}_{2(1-x)}\text{Gd}_{2x}\text{Se}_3$  was recorded at various temperatures for  $\mathbf{B} \parallel c$  axis. Figure 1 shows the EPR spectra at 300 and 4.2 K, exhibiting seven allowed transitions corresponding to  $\Delta M = \pm 1$ . The peak-to-peak average width of the first-derivative line shape at room temperature was about 60 G, decreasing to 40 G at 4.2 K. The line shapes

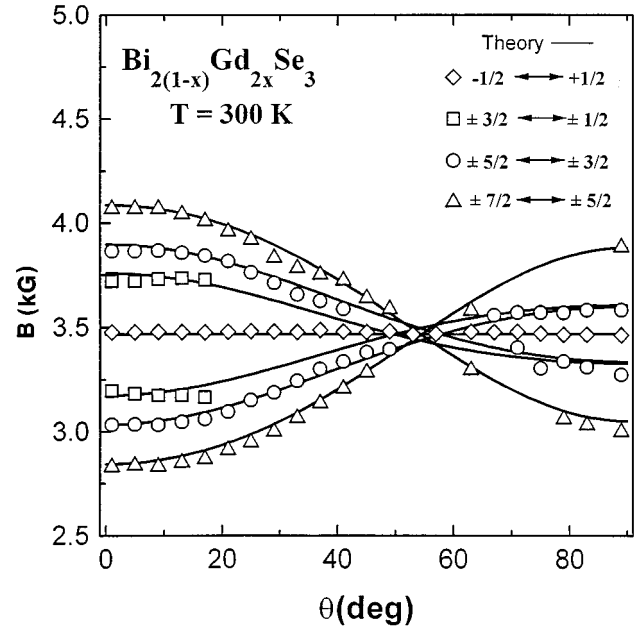


FIG. 2. Angular variation of the positions of the allowed  $\text{Gd}^{3+}$  fine-structure EPR lines ( $\Delta M = \pm 1$ ) at 300 K in  $\text{Bi}_{2(1-x)}\text{Gd}_{2x}\text{Se}_3$ , the external magnetic-field orientation being parallel to the  $c$  axis ( $\theta = 0^\circ$ ). Discrete symbols exhibit experimental data, while the solid lines represent calculated line positions.

of the observed transitions were Dysonian due to the skin effect caused by the high conductivity of the material.<sup>16,18</sup> Electrical-transport measurements at room temperature revealed that the sample was a  $n$ -type superconductor with carrier concentration  $n = 2.1 \times 10^{19}$  and resistivity  $\rho = 4.8 \times 10^{-4} \Omega \text{ cm}$ . The observed increase in the intensities of the lines at 4.2 K at low fields compared to those at high fields relative to the intensities at 300 K yielded the absolute signs  $b_2^0 < 0$ ,  $b_4^0 > 0$ , and  $b_6^0 < 0$ .<sup>15</sup> As a result of the rather large linewidth (4 mT) which masked this variation, it was very difficult to estimate the values of the parameters  $b_6^3$  and  $b_6^6$ , which are responsible for expected small variation of line position for  $\mathbf{B} \perp c$  axis with good accuracy. The values of all parameters, except for  $b_6^3$  and  $b_6^6$ , as estimated from line positions at 300 and 4.2 K are listed in Table I. In Fig. 2 are exhibited the EPR line positions in  $\text{Bi}_{2(1-x)}\text{Gd}_{2x}\text{Se}_3$  at various orientations of  $\mathbf{B}$ . Figure 3 shows a plot of the values of the spin-Hamiltonian parameters  $b_2^0$ ,  $b_4^0$ , and  $b_6^0$  as functions of temperature, similar to that observed in  $\text{KZnF}_3$  and  $\text{PbGdTe}$ .<sup>19,20</sup> The temperature variations of  $b_m^0$ ,  $m=2,4,6$ , were fitted theoretically to the following nonlinear expression in temperature:<sup>21</sup>

$$b_m^0(T) = b_m^0(0)[1 - CT^n]. \quad (2)$$

TABLE I. Fine-structure spin-Hamiltonian parameters for  $\text{Gd}^{3+}$  in  $\text{Bi}_{2(1-x)}\text{Gd}_{2x}\text{Se}_3$  single crystal at 300 and 4.2 K. Here  $\Delta$  represents the overall splitting in zero magnetic field  $\Delta = 12b_2^0 - 2b_4^0 + 6b_6^0$ .

$T$ (K)	$g$	$b_2^0$ (GHz)	$b_4^0$ (GHz)	$b_4^3$ (GHz)	$b_6^0$ (GHz)	$\Delta$ (GHz)
300	$2.001 \pm 0.005$	$-0.293 \pm 0.004$	$0.0052 \pm 0.0004$	$0.0033 \pm 0.0001$	$-0.0066 \pm 0.0004$	$-3.57 \pm 0.049$
4.2	$1.998 \pm 0.005$	$-0.349 \pm 0.01$	$0.011 \pm 0.0002$	$0.0031 \pm 0.0002$	$-0.015 \pm 0.0002$	$-4.35 \pm 0.12$

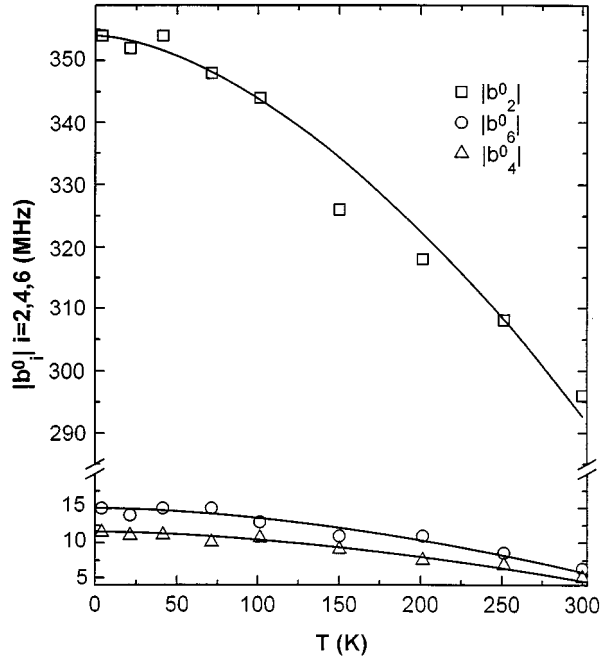


FIG. 3. The spin-Hamiltonian parameters  $b_2^0$ ,  $b_4^0$ , and  $b_6^0$  plotted as functions of temperature for  $\text{Gd}^{3+}$  in  $\text{Bi}_2\text{Se}_3$ . Discrete symbols exhibit data, while the solid lines are those calculated by use of Eq. (2).

Here  $b_m^0(0)$  and  $b_m^0(T)$  are the values of the parameter  $b_m^0$  at 0 K and  $T$ , respectively, with  $b_m^0(0)$  assumed to have the same value as that at 4.2 K. The  $[C, n]$  are  $[1.5, 1.64]$ ,  $[5.0, 1.65]$ , and  $[4.6, 1.69]$ , respectively, for  $b_2^0$ ,  $b_4^0$ , and  $b_6^0$ .

The coefficient  $\alpha$  that represents the admixture between the  $^8S_{7/2}$  and  $^6P_{7/2}$  states has been estimated as 0.12 from the  $g$  value as follows:<sup>15,20</sup>

$$g = (1 - g\alpha^2)g_S + \alpha^2g_P, \quad (3)$$

with  $g_S = 2.0023$  and  $g_P = 1.716$  being the Landé factor for the  $^8S_{7/2}$  and  $^6P_{7/2}$  states, respectively, and  $g = 1.998$  as estimated presently at 4.2 K.

## B. $\text{Gd}^{3+}$ in $\text{PbSe}$

### 1. Spin Hamiltonian

The  $^8S_{7/2}$  state of the gadolinium ion splits in the octahedral site symmetry of  $\text{PbSe}$  into two doublets  $\Gamma_6$  and  $\Gamma_7$  and one quadruplet  $\Gamma_8$ , which lies between the two doublets. The  $\Gamma_6$  state belongs to the lowest energy leading to a positive sign of the spin-Hamiltonian parameter  $b_4^0$ .<sup>1,15</sup> The  $\text{Gd}^{3+}$  spin Hamiltonian in cubic site symmetry is, in the usual notation and including the hyperfine interaction<sup>15-17</sup>

$$\mathcal{H} = g\mu_B \mathbf{B} \cdot \mathbf{S} + \frac{1}{60}b_4(O_4^0 + 5O_4^4) + \frac{1}{1260}b_6(O_6^0 - 21O_6^4) + \mathbf{A} \cdot \mathbf{I} \cdot \mathbf{S}. \quad (4)$$

### 2. EPR spectra

No EPR spectra could be observed at 300 K due to the skin effect, which eliminates the signal entirely. Figure 4(a) shows the EPR spectra of  $\text{Gd}^{3+}$  in  $\text{Pb}_{1-x}\text{Gd}_x\text{Se}$  at 4.2 K,

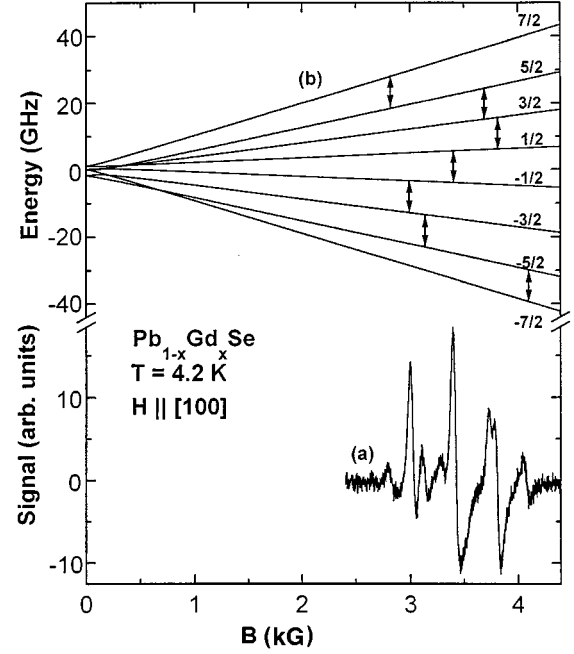


FIG. 4. (a) Plots of the  $\text{Gd}^{3+}$  EPR spectrum at 4.2 K in a single crystal of  $\text{Pb}_{1-x}\text{Gd}_x\text{Se}$  ( $x \sim 0.01$ ) and (b) the energy levels as calculated by a numerical diagonalization of the spin-Hamiltonian matrix as functions of the intensity of the external magnetic field, whose orientation is parallel to the  $[100]$  direction.

while Fig. 4(b) shows the transitions between the energy levels corresponding to the EPR lines in Fig. 4(a).

At low temperatures, the central transition splits into four hyperfine transitions corresponding to  $(2I+1)$  components of the nuclear magnetic moment of the  $^{155}\text{Gd}$  isotope. The gadolinium ion has two isotopes  $^{155}\text{Gd}$  and  $^{157}\text{Gd}$ , with non-zero nuclear magnetic moments 0.32 (abundance 14.8%) and 0.24 (abundance 15.6%), respectively, each characterized by

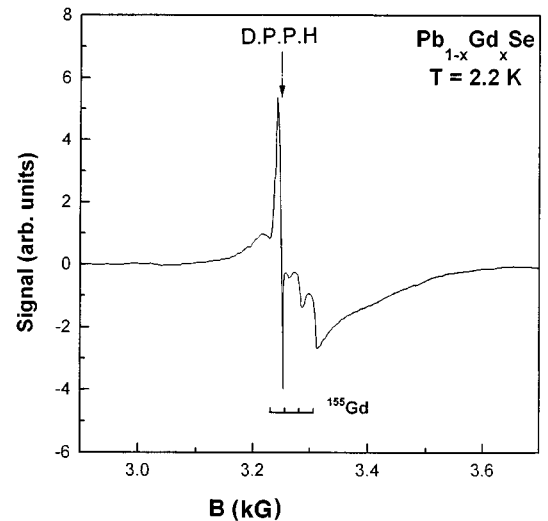


FIG. 5.  $\text{Gd}^{3+}$  EPR spectrum in  $\text{Pb}_{1-x}\text{Gd}_x\text{Se}$  powder at 2.2 K. The central  $+1/2 \leftrightarrow -1/2$  transition for the  $^{155}\text{Gd}$  and  $^{157}\text{Gd}$  isotopes (for each isotope  $I=3/2$ ) splits clearly into four hyperfine transitions. However, the lines corresponding to the two isotopes cannot be distinguished from each other due to the rather large linewidths.

the nuclear spin  $I=3/2$ . The hyperfine (HF) interaction constant parameter  $A$  can be estimated from the HF splitting of the fine-structure central line ( $M=+1/2 \leftrightarrow -1/2$ ): ( $m=-3/2, -1/2, +1/2, +3/2$ ;  $m$  is the nuclear magnetic quantum number). From Fig. 5, displaying the X band (9.14 GHz) spectrum at 2.2 K, the hyperfine-coupling constant  $A$  was estimated to be  $2.55 \pm 0.1$  mT, the average of the HF constants for the isotopes  $^{155}\text{Gd}$  and  $^{157}\text{Gd}$ , due to the non-resolution of the corresponding HF lines. The values of the fine-structure spin-Hamiltonian parameters as estimated from EPR line positions are  $g=1.990 \pm 0.005$ ,  $b_4=+92.0 \pm 2$  MHz, and  $b_6=-1.0 \pm 2$  MHz at 4.2 K, the value of the admixture parameter  $\alpha$  being 0.12 at 4.2 K as estimated by the use of Eq. (3).

#### IV. CONCLUDING REMARKS

From the present EPR measurements, it can be concluded that the  $\text{Gd}^{3+}$  ion substitutes at sites of hexagonal and octa-

hedral symmetries in  $\text{Bi}_2\text{Se}_3$  and  $\text{PbSe}$ , respectively. The spin-Hamiltonian parameters in  $\text{Bi}_2\text{Se}_3$  were found to be temperature dependent; the  $|b_2^0|$  value increased nonlinearly with decreasing temperature, attaining a constant value below 40 K. The EPR line shapes were Dysonian due to the high conductivity of the materials. The  $\text{Gd}^{3+}$  EPR spectrum, exhibiting hyperfine structures due to  $^{155}\text{Gd}$  and  $^{157}\text{Gd}$  isotopes, was observed in  $\text{PbSe}$  only at 2.2 K.

#### ACKNOWLEDGMENTS

We are grateful to Dr. F. Rachdi (GDPC) Université Montpellier (II) and Professor Y. Shapira (Tufts University, Boston) for helpful discussions, and to V. D. Ribes for technical assistance. This work was supported by CNRS, France (X.G., S.I., S.C., C.F., M.A., M.F., and J.C.T.), Natural Sciences and Engineering Research council of Canada (S.K.M., and S.I.) and the Polish Committee for Scientific Research (Z.G.).

\*Present address, Department of Physics, Concordia University, 1455 de Maisonneuve Boulevard West, Montreal, Quebec, H3G 1M8, Canada.

<sup>1</sup>S. Isber, S. Charar, V. Mathet, C. Fau, M. Averous, and Z. Golacki, Phys. Rev. B **52**, 1678 (1995).

<sup>2</sup>V. Bindilatti, N. F. Oliveira, Jr., Y. Shapira, G. H. McCabe, T. M. Liu, S. Isber, S. Charar, M. Averous, E. J. McNiff, Jr., and Z. Golacki, Phys. Rev. B **53**, 5472 (1996).

<sup>3</sup>G. B. Martins, M. A. Pires, G. E. Barberis, C. Rettori, and M. S. Torikachvili, Phys. Rev. B **50**, 14 822 (1994).

<sup>4</sup>M. Averous, C. Fau, S. Charar, M. El Kholdi, V. D. Ribes, and Z. Golacki, Phys. Rev. B **47**, 10 261 (1993).

<sup>5</sup>S. Isber, M. Averous, Y. Shapira, V. Bindilatti, A. N. Anisimov, N. F. Oliveira, Jr., V. M. Orera, and M. Demianiuk, Phys. Rev. B **51**, 15 211 (1995).

<sup>6</sup>S. Isber, S. Charar, V. Mathet, C. Fau, and M. Averous, Phys. Rev. B **51**, 15 578 (1995).

<sup>7</sup>M. El Kholdi, M. Averous, S. Charar, C. Fau, G. Brun, H. Ghomari-Bouanani, and J. Deportes, Phys. Rev. B **49**, 1711 (1994).

<sup>8</sup>D. L. Greenaway and G. Harbeke, J. Phys. Chem. Solids **26**, 1585 (1965).

<sup>9</sup>H. Scherrer, B. Hammou, J. P. Fleurial, and S. Scherrer, Phys. Lett. A **130**, 161 (1988).

<sup>10</sup>G. Martinez, M. Schluter, and M. L. Cohen, Phys. Rev. B **11**, 2 (1975).

<sup>11</sup>S. Charar, A. Obadi, C. Fau, M. Averous, V. D. Ribes, S. Dol corso, B. Liautard, J. C. Tedenac, and S. Brunet, Int. J. Infrared Millimeter Waves **17**, 365 (1996).

<sup>12</sup>W. Zawadzki, in *Physics of Narrow Gap Semiconductors*, Proceedings of the 4th International Conference on Physics of Narrow Gap Semiconductors, Linz, Austria, 1981, edited by E. Gornick, H. Heinrich, and L. Palmel-shofer (Springer, Berlin, 1982), Vol. 1.

<sup>13</sup>J. R. Anderson, G. Kido, Y. Nishina, M. Gorska, L. Kowalsky, and Z. Golacki, Phys. Rev. B **41**, 1014 (1990).

<sup>14</sup>G. B. Bacskey, P. J. Fensham, I. M. Ritchie, and R. N. Ruff, J. Phys. Chem. Solids **30**, 713 (1969).

<sup>15</sup>A. Abragam and B. Bleaney, *Electron Paramagnetic Resonance of Transition Metal Ions* (Clarendon, Oxford, 1970).

<sup>16</sup>C. P. Poole, Jr., *Electron Spin Resonance: A Comprehensive Treatise on Experimental Techniques* (Wiley-Interscience, New York, 1967).

<sup>17</sup>S. K. Misra, Magn. Reson. Rev. **10**, 285 (1985).

<sup>18</sup>M. Peter, D. Shaltiel, and J. H. Wernick, Phys. Rev. B **162**, B1395 (1962).

<sup>19</sup>M. Bartkowski, D. J. Nortcott, J. M. Park, A. M. Reddoch, and F. T. Hedgcock, Solid State Commun. **56**, 659 (1985).

<sup>20</sup>R. Lacroix, Helv. Phys. Acta **30**, 374 (1957).

<sup>21</sup>M. Walter, J. Walsh, L. Jeener, and N. Bloembergen, Phys. Rev. **162**, A1338 (1965).